

TiO₂ 나노입자를 이용한 고인장 PVC 필름 제조

엄원식 · 김영배 · 김성훈[†] · 한태희[†]

한양대학교 유기나노공학과

(2017년 5월 8일 접수, 2017년 7월 18일 수정, 2017년 7월 24일 채택)

High-Strain PVC Film Plasticized by TiO₂ Nanoparticles

Wonsik Eom, Young Bae Kim, Seong Hun Kim[†], and Tae Hee Han[†]

Department of Organic and Nano Engineering, Hanyang University, Seoul 04763, Korea

(Received May 8, 2017; Revised July 18, 2017; Accepted July 24, 2017)

초록: Tetrahydrofuran(THF)를 이용하여 제조한 poly(vinyl chloride)(PVC) 필름의 낮은 인장률과 인성이 TiO₂ 나노입자를 0.8 wt% 미만의 농도로 첨가하였을 때 향상되었다. 제조된 PVC/TiO₂ 복합재료는 383%의 우수한 인장률과 64.7 J m⁻³의 인성을 나타냈는데, 이는 PVC 고분자 사슬과 나노입자 사이에서 분자간 인력이 작용하였기 때문이다.

Abstract: The low strain and toughness of tetrahydrofuran (THF)-cast poly(vinyl chloride) (PVC) film were mitigated by introducing TiO₂ nanoparticles at loading below 0.8 wt%. The thus obtained PVC/TiO₂ composite showed superb elongation at break (383%) and toughness (64.7 J m⁻³) due to modified molecular interactions between nanoparticles and PVC chains.

Keywords: poly(vinyl chloride), TiO₂, inorganic nanofiller, high strain.

Introduction

Poly(vinyl chloride) (PVC) is one of the most important thermoplastics, combining low costs, good durability, and resistance toward chemical corrosion.^{1,2} In fact, pure PVC is hard, brittle, and stiff, being unsuited for commercial products such as films, shoes, and sap bags.^{3,4} Therefore, PVC is usually blended with large amount of plasticizers to achieve the desired flexibility and durability, with common examples including dialkyl phthalates, such as dioctyl phthalate (DOP) or bis(2-ethylhexyl) phthalate (DEHP).⁵ Moreover, the thermal instability of PVC in high-temperature processes such as extrusion can also be increased by using appropriate plasticizers.⁶ However, a large number of studies revealed that the DOP and DEHP are potential endocrine disruptors, being particularly harmful for infants and pregnant women.^{7,8} Therefore, finding alternative plasticizers or developing plasticizer-free processes is an import goal.^{9,10}

Nanoparticles have been reported to improve some mechan-

ical properties such as modulus and abrasion resistance.¹¹⁻¹³ For example, rubber particles make PVC films tougher but significantly reduce their tensile strength due to low hardness of organic filler.⁹ In contrast, inorganic nanofillers improve the toughness of PVC without the decreasing its tensile strength,¹⁰ as exemplified by the effect of common inorganic nanoparticles, such as calcium carbonate (CaCO₃) and titanium dioxide (TiO₂), on the mechanical properties of polymer matrix.^{14,15} The above nanoparticles are widely utilized to modify the viscosity of polymer solutions and the tensile strength of PVC.^{16,17} However, PVC still needs to be blended with conventional plasticizers to prevent its thermal degradation during extrusion.¹⁸

Herein, we have tried to develop a plasticizer-free process by investigating a model system at ambient conditions and thus neglecting the thermal instability of PVC. PVC was dissolved in tetrahydrofuran (THF), a common solvent, at room temperature and casted into a thin film, not requiring a high-temperature thermomechanical process. However, solvent-cast PVC films showed extremely low strain values (~14.6%) compared to those of PVC containing conventional plasticizer, DOP (131%). Therefore, we utilized nanoparticles as an efficient filler to improve the mechanical properties of PVC films,

[†]To whom correspondence should be addressed.
E-mail: than@hanyang.ac.kr; kimsh@hanyang.ac.kr
©2017 The Polymer Society of Korea. All rights reserved.

showing that their strain could be increased to 340% at low TiO₂ nanoparticle loading (<1.0 wt%).

Experimental

Materials. Solid PVC powders were supplied by Hanwha Chemical Co. Ltd. PVC had the degree of polymerization of 1600–1700 (as defined by JIS K 6720-2), particle sizes under 150 μm and an apparent specific gravity of 0.23 g cm⁻³, as defined by ASTM D 1895. TiO₂ nanoparticles of 5-, 25-, and 220-nm size were obtained from US Research Nanomaterials Inc., Evonik, and Cristal Global, respectively.

Film Casting. PVC and PVC/TiO₂ films were prepared as follows, PVC (3.4 g) was dispersed in THF (40 mL) to obtain a fully transparent solution using a roller mixer (Hwashin Instrument Co., Ltd., 205RMC), followed by addition of TiO₂ nanoparticles (0.2 wt%) and magnetic stirring for their homogeneous dispersion. Subsequently, the solution was poured in a glass dish to form a film. The solvent was slowly evaporated under low vacuum at 35 °C for 6 h to avoid bubbling, and the thus obtained film with an average thickness of 100 μm was washed several times with deionized water to remove THF residues.

Characterization. The mechanical properties of pristine PVC and PVC/TiO₂ films were tested using film stripes 100 μm thickness and 5 mm wide using a universal testing machine (5966, Instron) equipped with a 10 kN load cell operating at crosshead speed of 5.0 mm min⁻¹ and a gauge length of 20 mm. Interactions between TiO₂ and PVC polymer chains were investigated by thermogravimetric analysis (TGA; SDT Q600, TA Instruments) at temperatures of 25–600 °C and a heating rate of 10 °C min⁻¹ under air or nitrogen atmospheres. Glass transition temperatures (*T_g*) were determined by differential scanning calorimetry (DSC) at a heating rate of 10 °C min⁻¹ to characterize the effects of the casting method and TiO₂ addition. Fracture surfaces of PVC/TiO₂ films were characterized by scanning electron microscopy (SEM; NOVA Nano SEM 450) to confirm the improved elongation at break. Films were sputter-coated with platinum. Optical characterization was carried out at room temperature by ultraviolet-visible spectrophotometer (Perkin Elmer, Lambda 650S) in a wavelength range of 400–700 nm with an accuracy of 2 nm. Functional group analysis was performed by Fourier transform infrared spectroscopy (FTIR; Thermo Scientific, Nicolet 6700) in attenuated total reflectance (ATR) mode using 64 scans at a resolution of 2 cm⁻¹.

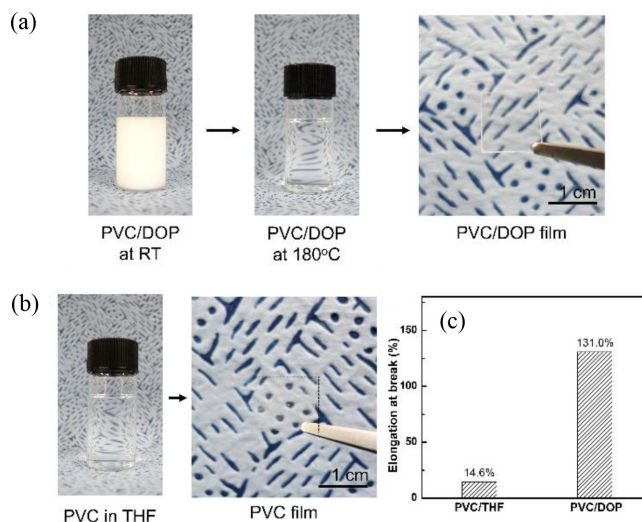


Figure 1. Production of conventionally plasticized (DOP) and THF-cast PVC films. Film preparation using (a) DOP (60 wt% PVC); (b) THF (2.8 wt% PVC), with film dimensions equaling 1.5×1.5 cm. The film was indicated with dashed line. (c) Elongation at break for commercially plasticized (DOP) and THF-cast films.

Results and Discussion

PVC powders were mechanically dispersed in DOP at room temperature, with the white color of the obtained mixture implying that PVC chains were not completely dissolved (Figure 1(a)).¹⁹ This above dispersion became transparent at 180 °C, as is often observed during PVC extrusion,²⁰ indicating that PVC chains were finally dissolved in DOP at high temperature. Thin transparent PVC films were casted in a glass dish (Figure 1(a)). Similarly, PVC powders were dissolved in THF at 85 mg mL⁻¹. Unlike for DOP, the above PVC solution was clear even at room temperature, implying the dissolution of PVC chains without the need to supply thermal energy (Figure 1(b)). Transparent PVC films could easily be obtained after evaporating the solvent. Figure 1(c) summarizes the strain properties of PVC films obtained using DOP as a conventional plasticizer and those cases from THF solution, revealing that the latter showed an extremely low elongation at break (14.6%) compared to that of the former (131%).

To understand this large difference in mechanical properties, the thermal behavior of the above films was investigated by TGA and DSC, as shown in Figure 2. In Figure 2(a) reveals that solvent-cast PVC film and PVC powder showed the significant weight losses around 270 and 420 °C, reflecting dechlorination (accompanied by stoichiometric elimination of HCl)²¹ and the conversion of C=C bonds to carbon dioxide, respec-

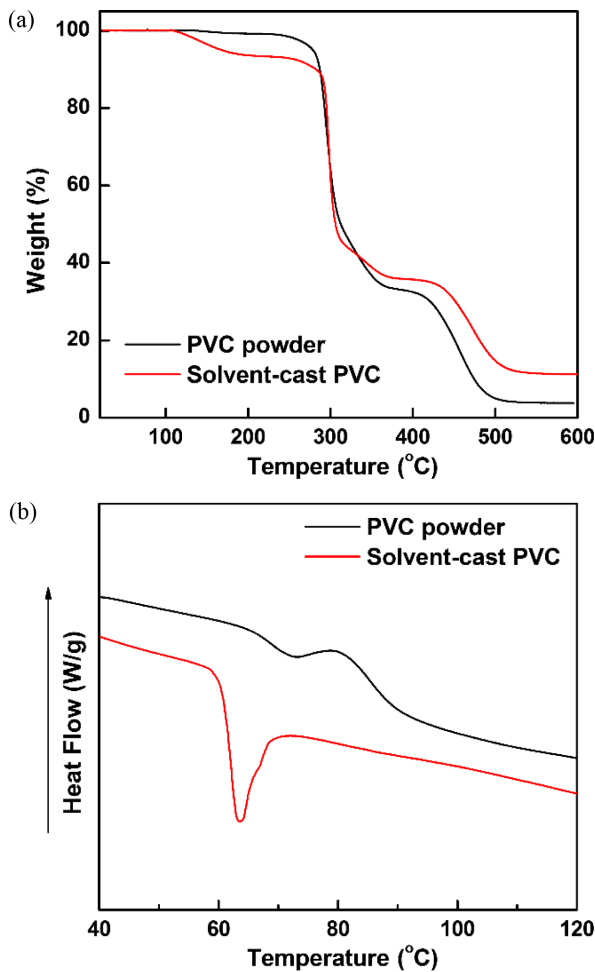


Figure 2. (a) TGA curves; (b) DSC curves of PVC powder and solvent-cast PVC.

tively.²¹ For solvent-cast PVC, an additional mass loss was observed at 114 °C due to the removal of trapped solvent.²² TGA results agreed with those obtained in the DSC study of raw PVC powders and solvent casted PVC film (Figure 2(b)), showing a clear decrease of T_g . This observation was explained by the presence of residual THF between polymer chains, which weakened interchain interactions and hindered chain entanglement, i.e., facilitates their disentanglement.²³ Subsequently, these solvent residues decreased T_g and became the major reason of deteriorated mechanical properties such as elongation at break and toughness.²³

This extremely low strain of THF-cast PVC films had to be enhanced for the practical applications, which was by adding TiO₂ nanoparticles to the PVC/THF solution. TiO₂ nanoparticles are commonly used for a wide range of applications related to color chemistry, cosmetics, and food industry owing to their non-toxicity.²⁴ At a low TiO₂ loading of 2 mg mL⁻¹, the

PVC solution became slightly opaque (Figure 3(a)), and the observed Tyndall effect indicated that TiO₂ nanoparticles were well dispersed without forming aggregates and phase-separation.²⁵ As showed in Figure 3(b), the introduction of TiO₂ nanoparticles reduced the transparency of PVC film in the visible region by ~10%.

To determine the efficacy of nanoparticles in enhancing the mechanical properties of PVC films, a systematic study was carried out for 5-, 25-, and 220-nm nanoparticles. Figure 3(c) clearly shows that neat PVC films were brittle, becoming ductile upon incorporation of TiO₂ nanoparticles with the content of 0.2 wt%. Introduction of 5-, 25-, and 220-nm nanoparticles increased the elongation at break to 39, 75, and 340%, respectively, with a value of 15% recorded for neat PVC films. Thus, the above value for 220-nm PVC/TiO₂ films exceeded that of neat PVC film 23-fold. Although the elongation at break values of PVC/TiO₂ composites were broadly variable, their tensile strength did not significantly depend on particle size, since inorganic nanoparticles like TiO₂ are known to toughen PVC composites without compromising their tensile strength (Table 1).¹⁰

These improvements in strain performance were closely related to the thermodynamic properties shown in Figure 3(d). DSC analysis revealed that all PVC/TiO₂ films with the content of 0.2 wt% TiO₂ exhibited lower T_g values than neat PVC films due to having higher thermal conductivity.²⁶ Even under identical heating conditions, the actual temperature of the films depends on their thermal conductivity. The T_g of PVC/TiO₂ films increased from 51 to 55 °C with increasing TiO₂ nanoparticle size, indicating improved polymer chain rigidity. The elongations at break values of PVC/TiO₂ composites were broadly variable, depending on particle size. According to Zeng *et al.*, the single-notched impact strength, elongation at break, and tensile properties of PVC/CaCO₃ nanocomposite were largely enhanced due to the well-dispersibility of nanoparticles in polymeric matrix.¹⁶

Figure 3(e) shows the FTIR spectra of PVC, TiO₂, and PVC/TiO₂ films. Pristine TiO₂ showed three characteristic major peaks at 3417, 1626, and 660 cm⁻¹, corresponding to surface hydroxyl groups, bending vibration of coordinated H₂O and Ti-OH, and Ti-O-Ti stretching vibrations, respectively.²⁷ The number of surface OH groups on TiO₂ was decreased by burying TiO₂ nanoparticles in the polymer matrix. Notably, the surface of these buried TiO₂ nanoparticles featured negatively charged oxygens that could be involved in hydrogen bonding with PVC chains.²⁸ Also, the positively charged TiO₂ has elec-

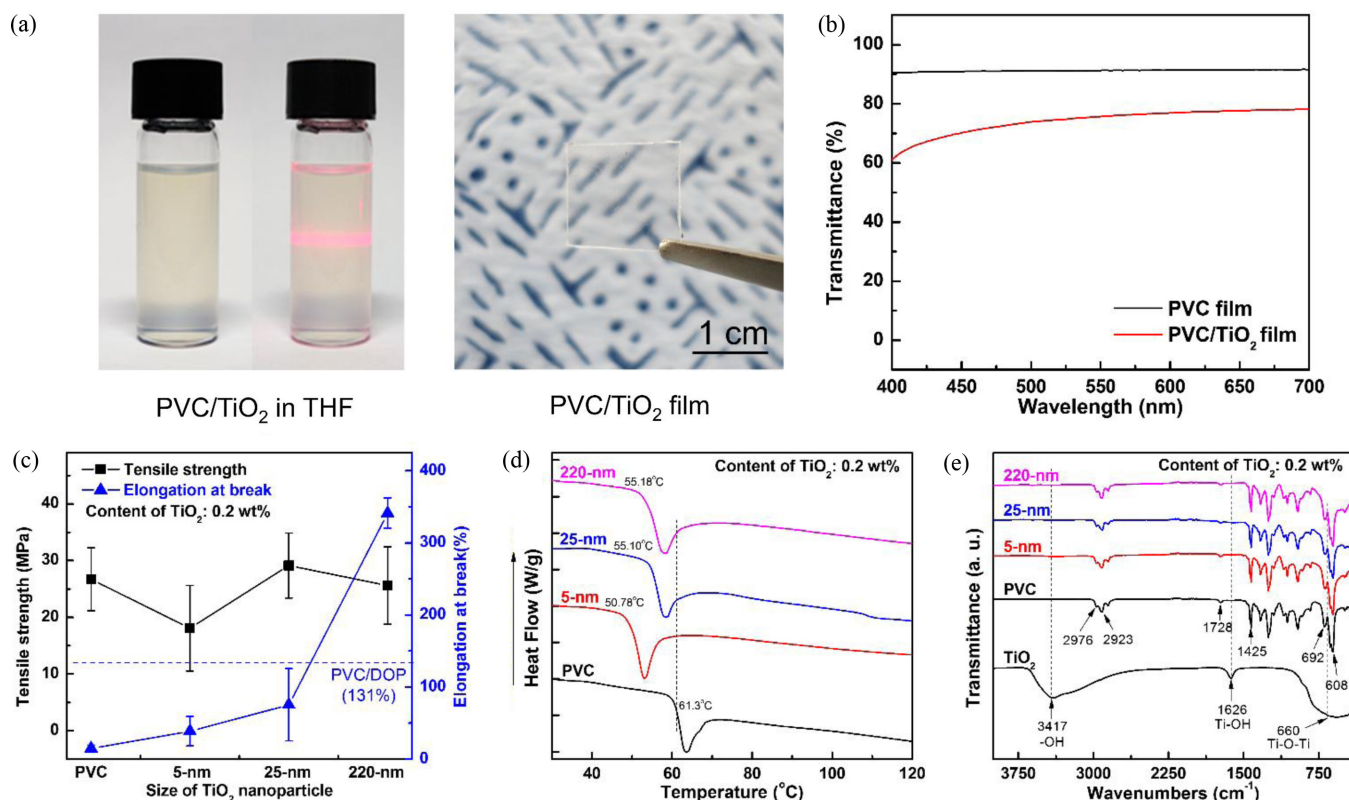


Figure 3. Effect of TiO₂ nanoparticle as PVC plasticizers. (a) Process for 1.5×1.5 cm PVC/TiO₂ films using 5-nm TiO₂ nanoparticles with the content of 2 mg mL⁻¹; (b) UV-vis absorption spectra of neat PVC and PVC/TiO₂ films containing 0.2 wt% 5-nm TiO₂ nanoparticles; (c) Tensile strength and elongation at break for PVC films containing 0.2 wt% TiO₂ nanoparticles of different size depending on TiO₂ nanoparticles inserted. (d) DSC curves; (e) FTIR spectra of PVC/TiO₂ films containing 0.2 wt% 5-, 25-, and 220-nm nanoparticles, respectively.

trostatic interactions with the negatively charged surface of PVC matrix in THF solution (pH 4.5~5.0). The Cl group of PVC and O group of TiO₂ are the sources of electrically charged surfaces.^{29,30}

To directly observe interactions between TiO₂ nanoparticles and the PVC matrix, we characterized the topologies of fractured film surfaces for different particle sizes (Figure 4). Whereas the rigid PVC film exhibited a smooth fracture surface (Figure 4(a)), PVC/TiO₂ nanocomposite films showed rough cross-sectional surfaces, except in the case of 5-nm TiO₂ nanoparticles (Figure 4(b)). The relatively low elongation at break and the smooth perforated fracture surface observed in the latter case indicate weak interfacial adhesion between 5-nm TiO₂ nanoparticles and the PVC matrix.¹⁴ On the other hand, the PVC/TiO₂ films containing 25- and 220-nm particles exhibited largely increased elongation at break and rough fracture surfaces, additionally featuring a number of voids around TiO₂ nanoparticles due to interfacial debonding (Figure 4(c) and 4(d)). A characteristic feature of these fracture surfaces

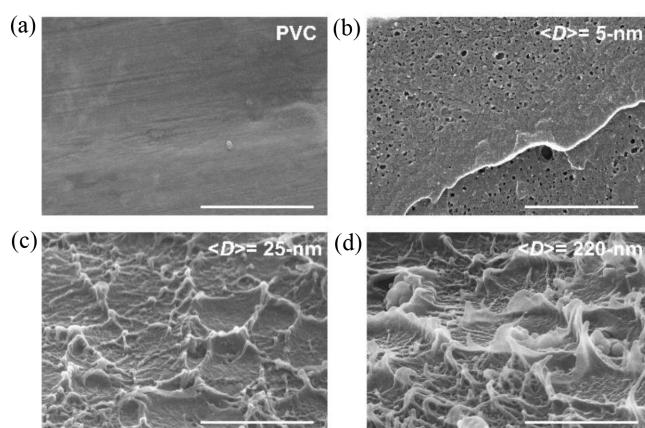


Figure 4. Fractured cross sections of (a) neat PVC; PVC/TiO₂ films containing (b) 5-nm; (c) 25-nm; (d) 220-nm TiO₂ particles. Scale bar=1 μm.

was the formation of thread-like striations,³¹ in agreement with the previously reported cavitation mechanism for rigid micro-particles.³² PVC/TiO₂ films containing 220-nm TiO₂ nanopar-

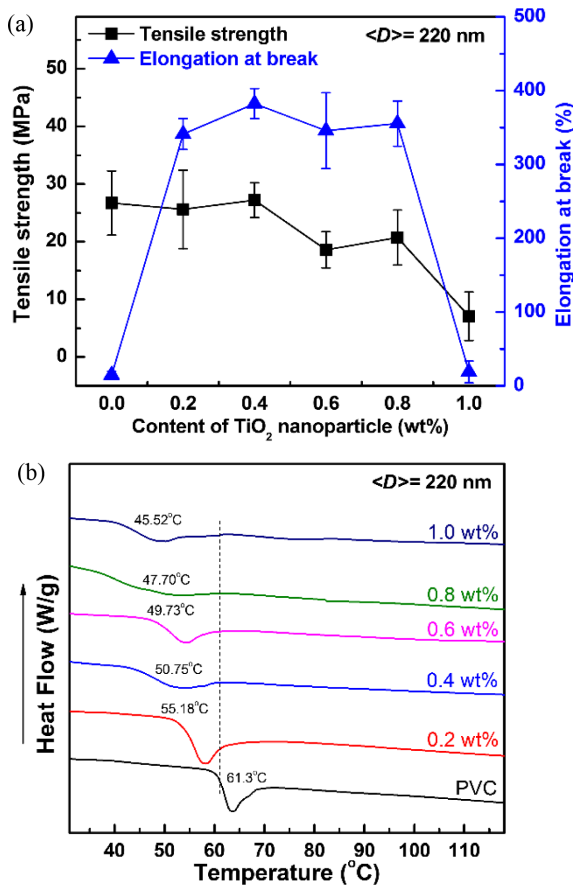


Figure 5. Effect of 220-nm TiO₂ nanoparticle loading concentration on the mechanical properties of PVC films: (a) tensile strength and elongation at break; (b) DSC curves.

ticles showed a rougher fracture surface, larger elongation, and higher T_g than those containing 25-nm nanoparticles.

The effect of nanoparticle content on mechanical properties was also examined (Figure 5(a)), revealing that the tensile

strength decreased with increasing the loading of 220-nm TiO₂ nanoparticles, implying the concomitant occurrence of moderate particle agglomeration.³³ However, upon increasing the loading of TiO₂ from 0.2 to 0.8 wt%, elongation at break and toughness significantly increased to above 340% and 45 J m⁻³, respectively (Table 1). However, at a higher TiO₂ content of 1.0 wt%, elongation at break, and toughness dramatically declined to 19% and 1.8 J m⁻³, respectively. Tensile strength decreased from about 20 to 7 MPa at a 1.0 wt% TiO₂ content. This behavior indicated that a content of 0.8 wt% corresponds to be percolation threshold concentration, above which the tensile strength, elongation at break, and toughness start to be significantly deteriorated. These changes could also be explained by studying the DSC behavior (Figure 5(b)) of neat and composite films continuously decreased, which was closely related to the decreased tensile strength and mechanical properties deterioration at the percolation threshold concentration.^{34,35}

Conclusions

Soft and organic plasticizer-free PVC films were prepared by dissolving PVC in THF and adding TiO₂ nanoparticles of various sizes at low loading levels. In the case of 220-nm particles, the obtained PVC/TiO₂ films showed an elongation at break (340%) more than 20 times larger than that of neat PVC film due to the nanoparticle chain adsorption effect. The improved tensile elongation at break and toughness were attributed to hydrogen bonding interactions and the polymer chain adsorption effect of TiO₂ nanoparticles. Increased TiO₂ loadings led to a gradual reduction of T_g , decreasing the tensile strength and deteriorating mechanical properties at the percolation threshold concentration.

Table 1. Physical and Mechanical Properties of PVC/TiO₂ Films

TiO ₂ particle diameter (nm)	TiO ₂ content (wt%)	Glass transition temperature (°C)	Tensile strength (MPa)	Elongation at break (%)	Toughness (J m ⁻³)
PVC	0	61.30	26.7	14.6	2.7
5	0.2	50.78	18.1	38.8	7.3
25	0.2	55.10	29.1	75.4	21.1
220	0.2	55.18	25.6	341.3	60.2
	0.4	50.75	27.2	382.5	64.7
	0.6	49.73	18.6	345.8	45.8
220	0.8	47.70	20.7	355.4	48.2
	1.0	45.52	7.1	18.8	1.8

Acknowledgments: TGA and DSC analyses were performed at the Electronics and Telecommunications Research Institute (ETRI). The SEM and FTIR were analyzed at Hanyang LINC Analytical Equipment Center (Seoul). This work was supported by “Civil research projects for solving social problems” through the National Research Foundation of Korea (NRF) funded by the Ministry of Science, ICT & Future Planning (2015M3C8A6A06014792).

References

1. Y. Du, J. Gao, J. Yang, and X. Liu, *Polym. Plast. Technol. Eng.*, **51**, 920 (2012).
2. J. Hu, X. Jia, C. Li, Z. Ma, G. Zhang, W. Sheng, X. Zhang, and Z. Wei, *J. Mater. Sci.*, **49**, 2943 (2014).
3. K. W. Li, *JCIIE*, **20**, 472 (2003).
4. H. Atkinson and S. Duffull, *J. Pharm. Pharmacol.*, **43**, 374 (1991).
5. J. R. Fried, *Polymer science and technology*, 2nd edition, Prentice Hall, Vicksburg, 2014.
6. S. Y. Soong, R. E. Cohen, and M. C. Boyce, *Polymer*, **48**, 1410 (2007).
7. S. Loff, F. Kabs, K. Witt, J. Sartoris, B. Mandl, K. Niessen, and K. Waag, *J. Pediatr. Surg.*, **35**, 1775 (2000).
8. J. A. Tickner, T. Schettler, T. Guidotti, M. McCally, and M. Rossi, *Am. J. Ind. Med.*, **39**, 100 (2001).
9. M. Moghbeli and S. Tolute, *J. Appl. Polym. Sci.*, **113**, 2590 (2009).
10. B. Yin and M. Hakkarainen, *J. Mater. Chem.*, **21**, 8670 (2011).
11. K. Yao, J. Gong, N. Tian, Y. Lin, X. Wen, Z. Jiang, H. Na, and T. Tang, *RSC Adv.*, **5**, 31910 (2015).
12. S. Hosseini, M. Askari, P. Koranian, S. Madaeni, and A. Moghadassi, *J. Ind. Eng. Chem.*, **20**, 2510 (2014).
13. J. Liu, H. Yan, and K. Jiang, *Ceram. Int.*, **39**, 6215 (2013).
14. X.-L. Xie, Q.-X. Liu, R. K.-Y. Li, X.-P. Zhou, Q.-X. Zhang, Z.-Z. Yu, and Y.-W. Mai, *Polymer*, **45**, 6665 (2004).
15. S. Horikoshi, N. Serpone, Y. Hisamatsu, and H. Hidaka, *Environ. Sci. Technol.*, **32**, 4010 (1998).
16. X. Zeng, W. Wang, G. Wang, and J. Chen, *J. Mater. Sci.*, **43**, 3505 (2008).
17. O. A. Harzallah and D. Dupuis, *Rheol. Acta*, **42**, 10 (2003).
18. E. Calò, A. Greco, and A. Maffezzoli, *Polym. Degrad. Stab.*, **96**, 784 (2011).
19. N. Nakajima, M. Sadeghi, and T. Kyu, *J. Appl. Polym. Sci.*, **41**, 889 (1990).
20. C. Wan, X. Qiao, Y. Zhang, and Y. Zhang, *J. Appl. Polym. Sci.*, **89**, 2184 (2003).
21. M. A. Da Silva, M. G. A. Vieira, A. C. G. Maçumoto, and M. M. Beppu, *Polym. Test.*, **30**, 478 (2011).
22. M. Hasan and M. Lee, *Prog. Nat. Sci.*, **24**, 579 (2014).
23. J. Chen, G. Xue, Y. Li, L. Wang, and G. Tian, *Macromolecules*, **34**, 1297 (2001).
24. S. M. Gupta and M. Tripathi, *Chin. Sci. Bull.*, **56**, 1639 (2011).
25. S. Lee, H. Park, U. Paik, and T. H. Han, *J. Solid State Chem.*, **224**, 76 (2015).
26. D. S. Fryer, R. D. Peters, E. J. Kim, J. E. Tomaszewski, J. J. de Pablo, P. F. Nealey, C. C. White, and W.-L. Wu, *Macromolecules*, **34**, 5627 (2001).
27. S. S. Mali, C. A. Betty, P. N. Bhosale, and P. Patil, *ECS J. Solid State Sci. Technol.*, **1**, M15 (2012).
28. S. Cho and W. Choi, *J. Photochem. Photobiol. A Chem.*, **143**, 221 (2001).
29. S. Matsuzawa, C. Maneerat, Y. Hayata, T. Hirakawa, N. Negishi, and T. Sano, *Appl. Catal. B*, **83**, 39 (2008).
30. H. Park and W. Choi, *J. Phys. Chem. B*, **108**, 4086 (2004).
31. D. Wu, X. Wang, Y. Song, and R. Jin, *J. Appl. Polym. Sci.*, **92**, 2714 (2004).
32. W. Zuiderduin, C. Westzaan, J. Huetink, and R. Gaymans, *Polymer*, **44**, 261 (2003).
33. Y. Thio, A. Argon, R. Cohen, and M. Weinberg, *Polymer*, **43**, 3661 (2002).
34. Z. Wang, J. Liu, S. Wu, W. Wang, and L. Zhang, *Phys. Chem. Chem. Phys.*, **12**, 3014 (2010).
35. S. Barrau, P. Demont, C. Maraval, A. Bernes, and C. Lacabanne, *Macromol. Rapid Commun.*, **26**, 390 (2005).